Organometallic Precursors for the Formation of GaN by MOCVD: Structural Characterization of (CH 3) 3 GaNH(CH 2 CH 3) 2 by Gas-Phase Electron Diffraction and ab Initio Molecular O…

ARTICLE *in* THE JOURNAL OF PHYSICAL CHEMISTRY A · SEPTEMBER 2002

Impact Factor: 2.69 · DOI: 10.1021/jp020523o

5 AUTHORS, INCLUDING:

Kirsten Aarset
Oslo and Akershus University College of Appl…
31 PUBLICATIONS **250** CITATIONS
SEE PROFILE

Kolbjørn Hagen
Norwegian University of Science and Techno…
102 PUBLICATIONS **1,147** CITATIONS
SEE PROFILE

David A. Rice
University of Reading
145 PUBLICATIONS **1,637** CITATIONS
SEE PROFILE

Organometallic Precursors for the Formation of GaN by MOCVD: Structural Characterization of $(CH_3)_3GaNH(CH_2CH_3)_2$ by Gas-Phase Electron Diffraction and ab Initio Molecular Orbital Calculations

Kirsten Aarset,[†] Carolyn E. Beer,[‡] Kolbjørn Hagen,[§] Elizabeth M. Page,*[,‡] and David A. Rice[‡]

Faculty of Engineering, Oslo University College, Cort Adelers Gate 30, N-0254 Oslo, Norway, Department of Chemistry, University of Reading, Whiteknights Park, Reading RG6 6AD, U.K., and Department of Chemistry, Norwegian University of Science and Technology, NTNU, N-7491 Trondheim, Norway

Received: February 26, 2002; In Final Form: June 18, 2002

The reaction of $(CH_3)_3Ga$ with $NH(CH_2CH_3)_2$ led to the formation of trimethylgallium diethylamine, $(CH_3)_3Ga{\cdot}NH(CH_2CH_3)_2$. The structure of $(CH_3)_3Ga{\cdot}NH(CH_2CH_3)_2$ was determined from gas-phase electron-diffraction data combined with results from ab initio molecular orbital and density functional theory calculations. A gauche-anti conformer was found where the two Ga−N−C−C torsional angles are $\phi_1 = 151(4)°$ and $\phi_2 = -100(4)°$. The average experimental bond distances (r_g) and bond angles ($\angle_\alpha$), with estimated 2σ uncertainties (σ include estimates of systematic errors and correlation in the experimental data) are r(C−H) = 1.116(3) Å, r(Ga−C) = 1.996(3) Å, r(Ga−N) = 2.204(12) Å, r(C−N) = 1.474(4) Å, r(C−C) = 1.544(4) Å, ∠N−Ga−C = 99.5(13)°, ∠Ga−N−C = 112.5(9)°, ∠N−C−C = 114.8(8)°, ∠C−N−C = 113.3(11)°, and ∠C−Ga−C = 117.3(7)°. Thermolysis of $(CH_3)_3Ga{\cdot}NH(CH_2CH_3)_2$ was studied, from which it was concluded that the compound is not a suitable precursor for the production of GaN in MOCVD.

Introduction

In recent years there has been much interest focused on the chemistry of species containing Ga−N bonds due to the potential use of such complexes as precursors to the wide band gap semiconductor GaN which is a type 13/15 semiconductor with high thermal, radiation, and chemical resistance. It therefore finds applications in high temperature and high power microelectronic and optoelectronic devices including passivation barriers, ohmic contacts in integrated circuits, and blue light emitting diodes.[1,2] Layers of GaN have been successfully produced by metal organic chemical vapor deposition (MOCVD) from precursors such as trimethylgallium and ammonia, which decompose thermally over a heated substrate leaving a layer of the desired material and gaseous side products.[3] However, the handling difficulties presented by the pyrophoric gallium trialkyls coupled with the high overpressures of ammonia at the high temperatures required have prompted research into the isolation of more accessible single-source precursors containing Ga−N bonds.

Intense activity in this area has resulted in a proliferation of complexes of trialkyl gallium with N-containing adducts that include amines,[4−11] hydrazines[14] and derivatives,[13] and azides.[12,15,16] Requirements of single-source precursors such as these are ease of handling, suitable volatility, thermal or photochemical decomposition at accessible temperatures, and high purity.

Adduct formation between ammonia and trimethylgallium is well documented.[17−19] The structure of the product $(CH_3)_3Ga{\cdot}NH_3$ has been studied in the vapor phase.[20] Thermal decomposition of the adduct was investigated and was found to result in the formation of a trimer $[(CH_3)_2GaNH_2]_3$ that was characterized by single-crystal analysis.[21] Similar behavior had previously been reported for the aluminum adduct $(CH_3)_3Al{\cdot}NH_3$, which decomposes at room temperature to trimeric $[(CH_3)_2AlNH_2]_3$ and exists as a dimer−trimer equilibrium in the vapor phase.[22,23]

Such oligomerizations, accompanied by evolution of an alkane, are not restricted to the ammonia adducts of the group 13 alkyls. Reaction of Bu^t_2GaCl with LiNHPh led to the formation of $[Bu^t_2Ga(\mu\text{-NHPh})]_2$, whose solid-state structure has been determined.[24] The reactions of $(CH_3)_3Ga$ with a range of secondary amines have been studied and the products investigated by standard spectroscopic techniques.[8,25] The vapor-phase structure of the dimethylamine adduct was determined by our group. Thermolysis of the adduct in a N_2 or Ar atmosphere resulted in methane formation and the production of the dimer $[(CH_3)_2Ga(\mu\text{-}N(CH_3)_2)]_2$, whose vapor-phase structure was also determined.[25]

It is apparent from work carried out to date that the vapor-phase behavior of these group 13 trialkyl complexes formed with amines and other N-containing species is not straightforward, neither are the routes to GaN. Metal−nitride layer formation is thought to proceed during chemical vapor deposition by successive displacement reactions of the alkyl group by ammonia or the amine, as illustrated below for the formation of GaN from $(CH_3)_3Ga$ and NH_3.

$$(CH_3)_3Ga + NH_3 \rightarrow (CH_3)_3Ga{\cdot}NH_3$$

$$3[(CH_3)_3Ga{\cdot}NH_3] \rightarrow 3CH_4 + [(CH_3)_2GaNH_2]_3$$

$$^n/_3[(CH_3)_2GaNH_2]_3 \rightarrow nCH_4 + [CH_3GaNH]_n$$

Knowledge of the gas-phase structures of these group 13 nitrogen ligand adducts is therefore pivotal in understanding the reactions that proceed in MOCVD. During the course of our investigations into the reactions of $(CH_3)_3Ga$ with N-

[†] Oslo University College.
[‡] University of Reading.
[§] Norwegian University of Science and Technology.

10.1021/jp020523o CCC: $22.00
Published on Web 08/15/2002

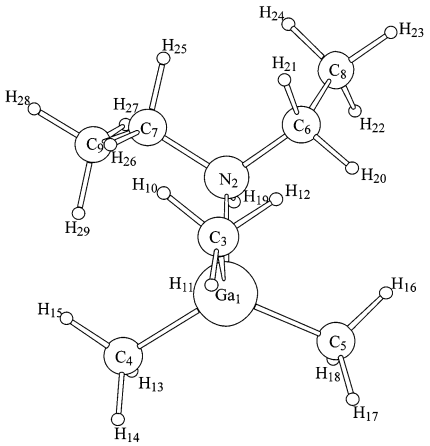

Figure 1. Diagram of the gauche-anti conformer of $Me_3Ga{\cdot}NHEt_2$ with atom numbering.

containing species we have isolated the 1:1 adduct $(CH_3)_3Ga{\cdot}NEt_2H$ (Figure 1), and presented here are the results from a gas-phase electron diffraction and spectroscopic study of the complex. The behavior of the complex upon thermolysis was also studied to assess its potential as a precursor for GaN formation in MOCVD.

Experimental Section

Preparation of $(CH_3)_3Ga{\cdot}NHEt_2$. Standard high vacuum line techniques and an oxygen-free nitrogen-filled drybox were employed in the handling and storage of samples. Trimethylgallium was kindly supplied by Professor D. J. Cole-Hamilton and was distilled in vacuo before use. Diethylamine was dried over barium oxide and distilled and stored on grade 4 Å molecular sieves prior to use. The sample of $Me_3Ga{\cdot}NHEt_2$ was prepared by mixing equimolar quantities of the amine and trimethylgallium as described previously.[25] A slight excess of the amine was used, which was removed after reaction by evaporation on the vacuum line. The product was obtained as a colorless liquid with a vapor pressure of around 1 Torr at room temperature.

Physical Methods. Infrared spectra of $(CH_3)_3Ga{\cdot}NHEt_2$ were measured in the gas phase at room temperature in a 10 cm path-length cell fitted with KI windows using a Perkin-Elmer 1720X Fourier transform instrument. Solid-phase spectra were recorded at 77 K on a Perkin-Elmer 983 dispersive spectrometer; both instruments have a resolution of ± 1 cm $^{-1}$. Fourier transform Raman spectra were recorded in the liquid phase on a modified Perkin-Elmer 1710 FT-IR spectrometer using the 1064 nm line of a Nd:YAG laser. Mass spectra were obtained by means of a quadrupole Vacuum Generators SXP800 Spectramass instrument. ^{1}H NMR spectra were recorded at 200 MHz using a Varian T60 spectrometer.

Gas-Phase Electron Diffraction. Gas-phase electron diffraction data of $Me_3Ga{\cdot}NHEt_2$ were obtained on the Balzers Eldigraph KDG-2 apparatus at the University of Oslo.[26] The nozzle-to-plate distances were 496.73 and 246.81 mm and data collection was performed with both the nozzle and the sample at room temperature. The electron wavelength (0.058 69 Å) was calibrated against diffraction patterns of benzene. Six plates from the long and five plates from the short-camera distance experiments were selected for use in the structure analysis. Optical densities were measured on a Joyce Loebl microdensitometer at the University of Oslo, and the data were reduced in the usual way.[27] The ranges of data were $2.00 \le s/\text{Å}^{-1} \le 15.00$ and $4.00 \le s/\text{Å}^{-1} \le 27.00$; the data interval was $\Delta s = 0.25$ Å^{-1}. A calculated background was subtracted from the data for each plate to yield experimental intensity curves in the form $sI_m(s)$. The intensity curves with backgrounds are shown in Figure 2. An experimental radial distribution (RD) curve was calculated from the average modified molecular intensity curve $I'(s) = sI_m(s)Z_{Ga}Z_C(A_{Ga}A_C)^{-1} \exp(-0.002s^2)$, where $A = s^2F$ and F is the absolute value of the complex electron scattering amplitudes. Theoretical intensity data were used for the unobserved region $s \le 1.75$ Å^{-1}. The scattering amplitudes and phases were taken from tables.[28] The intensity data and final backgrounds are available as Supporting Information in Tables 1S and 2S.

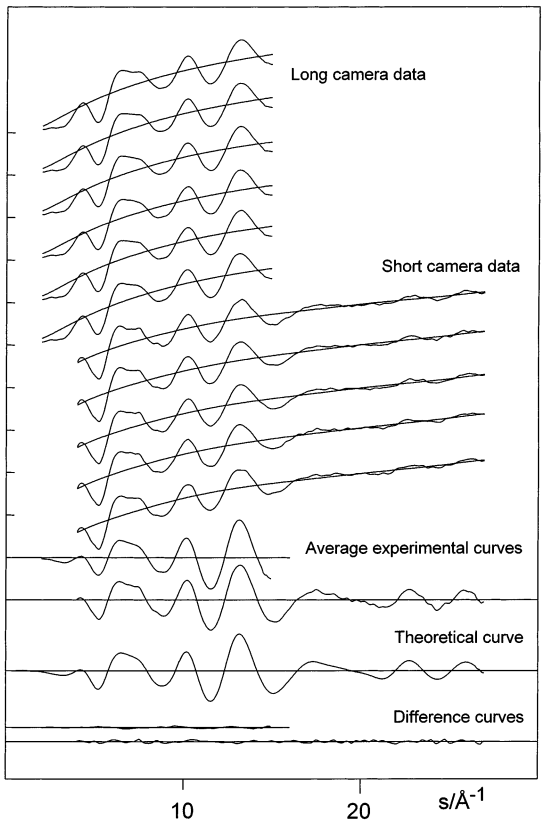

Figure 2. Intensity curves for $Me_3Ga{\cdot}NHEt_2$. Long camera and short camera curves are magnified eight times relative to the backgrounds on which they are superimposed. Average curves are in the form $sI_m(s)$. The theoretical curve is calculated from the final model shown in Tables 1 and 2. Difference curves are experimental minus theoretical.

Molecular Orbital Calculations. Ab initio molecular orbital calculations at the HF/6-311+G(d) level, using the Gaussian94 program[29] indicated that an anti-gauche (AG) form with C_1 symmetry was a conformational minimum with $\phi_1(\text{Ga}-\text{N}-\text{C}_6-\text{C}_8) = 156°$ and $\phi_2(\text{Ga}-\text{N}-\text{C}_7-\text{C}_9) = -90°$. Second-order Möller−Plesset (MP2) and density functional theory (B3LYP) calculations were also carried out and a single conformational minimum was found in these calculations. The results obtained from these calculations for some important geometrical parameters for $Me_3Ga{\cdot}NHEt_2$ are shown in Table 1.

Normal Coordinate Calculations. Vibrational quantities are an important part of the model used to analyze the experimental data. Ab initio frequency calculations at the HF/6-311+G(d) level gave us a theoretical force field for the molecular vibrations. This theoretical force field was scaled, using the ususal scale constants for HF-calculated force fields, and the scaled force constants were used to calculate vibrational amplitudes, perpendicular amplitude corrections, and centrifugal distortions, using the ASYM40 program.[30] These vibrational

TABLE 1: Parameter Values for $Me_3Ga{\cdot}NHEt_2$[a]

	ED	HF[b]	MP2[c]	B3LYP[b]
r(N−H)	[1.001]	1.001	1.013	1.019
r(C−H)[d]	1.092(3)	1.087	1.095	1.095
r(C−N)[d]	1.460(4)	1.478	1.484	1.489
r(C−C)[d]	1.510(4)	1.523	1.521	1.526
r(Ga−C)[d]	1.974(3)	2.017	2.014	2.014
r(Ga−N)	2.201(12)	2.247	2.180	2.246
∠N−Ga−C_3	98.9(13)	100.3	99.1	100.1
∠N−Ga−C_4	102.8(13)	104.2	104.2	104.4
∠N−Ga−C_5	96.8(13)	98.2	98.1	97.6
∠Ga−N−C_6	109.6(9)	108.9	108.5	108.6
∠Ga−N−C_7	115.5 (9)	114.8	113.7	114.9
∠C−N−C	113.3(11)	113.3	112.6	113.3
∠N−C_6−C_8	115.8(8)	114.2	113.4	114.6
∠N−C_7−C_9	113.9(8)	112.3	111.2	112.2
∠Ga−C−H[d]	110.6(10)	112.1	112.0	112.0
∠N−C−H[d]	[109.0][e]	109.0	108.6	109.3
∠C−C−H[d]	[111.1][e]	111.1	111.3	111.3
∠Ga−N−H	[102.9][e]	102.9	105.6	103.2
ϕ(C_3−Ga−N−H)	176(8)	164.1	164.3	163.1
ϕ(Ga−N−C_6−C_8)	151(4)	156.0	157.7	158.0
ϕ(Ga−N−C_7−C_9)	−100(4)	−90.4	−90.6	−88.1
ϕ(N−C_6−C_8−H)	[180.2][e]	180.2	180.7	180.0
ϕ(N−C_7−C_9−H)	[177.6][e]	177.6	176.2	177.1
ϕ(N−Ga−C−H)	[173.5][e]	173.5	170.6	174.5

[a] Distances are in Ångstroms, angles in degrees. Experimental values are r_α and $\angle_\alpha$. Uncertainties are 2σ and include estimates of systematic errors and correlation in the experimental data. [b] Basis set used: 6-311+G(d). [c] Basis set used: 6-311G(d). [d] Average value. [e] Value was not refined.

quantities were used to convert the r_a distances used in the electron diffraction model to the geometrically consistent r_α distances.

Structure Analysis. The molecule $Me_3Ga{\cdot}NHEt_2$ is depicted in Figure 1, which also shows the atomic numbering scheme. By setting the differences between the symmetrically nonequivalent C−N and C−C distances and the N−Ga−C, Ga−N−C, and N−C−C angles at the values obtained from HF/6-311G(d) values, we can define the geometry of $Me_3Ga{\cdot}NHEt_2$ by six distance and fifteen angle parameters, in our model taken as r(Ga−N), r(C−N), r(C−H), r(N−H), r(Ga−C), r(C−C), ∠Ga−N−C, ∠N−C−C, ∠N−C−H, ∠H−$C_{6,7}$−H, ∠C−C−H, ∠Ga−N−H, ∠N−Ga−C, ∠Ga−C−H, ∠C−N−C, ϕ(Ga−N−C_6−C_8), ϕ(Ga−N−C_7−C_9), ϕ(N−C_6−C_8−H), ϕ(N−C_7−C_9−H), ϕ(N−Ga−C−H), and ϕ(H−N−Ga−C_3). Only an average C−H distance was used as a parameter, and C_{3v} symmetry was assumed for the methyl groups. Amplitude parameters were constructed by grouping the individual vibrational amplitudes. The nature of the groups can be seen in the table of the final results (Table 2). A trial structure was constructed from the experimental radial distribution curve by incorporating the results from the theoretical calculations and parameter values for related molecules. The structure was defined in terms of the geometrically consistent r_α-type distances. These were converted to the r_a-type required by the formula for the scattered intensities by using values of centrifugal distortion constants (δr), perpendicular amplitude corrections (K), and root-mean-square amplitudes of vibration (l). Least squares refinements of this structure were carried out,[31] adjusting a theoretical $sI_m(s)$ curve simultaneously to the eleven experimental data sets (one from each photographic plate), using a unit weight matrix.

The most stable conformation for the Ga−N−C−C chain was considered originally to be the AA form. Thus initial refinements were carried out with the ethyl groups fixed in the anti conformation ($\phi_1 = \phi_2 = 180°$). However, refinements on this model resulted in the distances between terminal CH_3 groups being unreasonably small, which would force one of the Ga−N−C−C angles to adopt the gauche conformation. Further refinements carried out on an AG conformer with starting values for ϕ_1(Ga−N−C_6−C_8) and ϕ_2(Ga−N−C_7−C_9) torsion angles (156.0° and −90.4°, respectively) taken from the molecular orbital calculations (HF/6-311+G(d)) yielded good agreement between the experimental and theoretical intensity curves. A further refinement was carried out using a model consisting of a conformational mixture of the GG and AA forms. Though the fit of this model to the data was acceptable, it was not as good as the fit obtained for the simple AG conformer. Thus the AG conformer was concluded to be the stable form of $(CH_3)_3Ga{\cdot}NHEt_2$, an observation that is in agreement with results from the ab initio calculations and is reinforced by subsequent refinements. Not all the parameters involving the positions of hydrogen atoms could be determined experimentally and so these parameters were kept constant at the values calculated. In the final least squares refinement, five distance parameters, seven angle parameters, and three amplitude parameters were refined simultaneously. The most important values for the parameters obtained from this refinement are shown in Table 1 where the relevant results from a number of the theoretical calculations are also shown. In Table 2 some of the interatomic distances are given together with values for the

TABLE 2: Experimental Values for Atom Distances and rms Vibrational Amplitudes in $Me_3Ga{\cdot}NHEt_2$[a]

	r_α	r_g	l_{calcd}	l_{exp}
r(N−H)	[1.001][c]	[1.025][c]	0.073	
r(C−H)[b]	1.092(3)	1.116	0.080	
r(Ga−C_3)	1.973(3)	1.993	0.059	0.063(5)
r(Ga−C_4)	1.974(3)	1.995	0.059	0.063(5)
r(Ga−C_5)	1.976(3)	1.999	0.059	0.063(5)
r(Ga−N)	2.201(12)	2.204	0.103	
r(N−C_6)	1.459(4)	1.473	0.051	
r(N−C_7)	1.461(4)	1.476	0.051	
r(C_6−C_8)	1.512(4)	1.539	0.052	
r(C_7−C_9)	1.508(4)	1.549	0.052	
r(Ga···C_6)	3.020(12)	3.027	0.116	0.130(19)
r(Ga···C_7)	3.122(11)	3.129	0.132	0.145(19)
r(Ga···C_8)	4.387(20)	4.397	0.129	0.143(19)
r(Ga···C_9)	3.992(44)	4.006	0.183	0.194(19)
r(N···C_8)	2.517(10)	2.540	0.070	
r(N···C_9)	2.489(10)	2.518	0.070	
r(N···C_3)	3.174(30)	3.186	0.134	0.109(14)
r(N···C_4)	3.266(29)	3.279	0.155	0.128(14)
r(N···C_5)	3.128(31)	3.142	0.146	0.120(14)
r(C_3···C_4)	3.363(15)	3.392	0.125	0.100(14)
r(C_3···C_5)	3.401(12)	3.431	0.123	0.098(14)
r(C_4···C_5)	3.353(14)	3.386	0.122	0.098(14)
r(C_3···C_6)	3.476(101)	3.493	0.217	
r(C_3···C_7)	3.666(105)	3.675	0.257	
r(C_4···C_6)	4.545(21)	4.550	0.125	
r(C_4···C_7)	3.608(84)	3.630	0.216	
r(C_5···C_6)	3.398(110)	2.417	0.191	
r(C_5···C_7)	4.483(26)	4.487	0.144	
r(C_6···C_7)	2.439(15)	2.463	0.070	
r(C_8···C_9)	4.004(82)	4.033	0.250	
r(C_6···C_9)	3.633(28)	3.662	0.105	
r(C_7···C_8)	3.189(37)	3.221	0.110	
r(C_3···C_8)	4.986(99)	4.999	0.225	
r(C_3···C_9)	4.917(134)	4.927	0.258	
r(C_4···C_8)	5.721(47)	5.725	0.159	
r(C_4···C_9)	3.800(113)	3.837	0.212	
r(C_5···C_8)	4.432(96)	4.453	0.263	
r(C_5···C_9)	5.237(101)	5.245	0.287	

[a] Distances (r) and amplitudes (l) are in Ångstroms. Values in parentheses are 2σ and include estimates of uncertainties in camera height and electron wavelength. [b] Average value. [c] Value was not refined.

TABLE 3: Correlation Matrix (×100) for Parameters of $Me_3Ga{\cdot}NHEt_2$

	$100\sigma_{LS}$[a]	r_1	r_2	r_3	r_4	r_5	r_6	r_7	$\angle_8$	$\angle_9$	$\angle_{10}$	$\angle_{11}$	$\angle_{12}$	l_{13}	l_{14}	
r(Ga−N)	0.42	100														
r(C−N)	0.12	−31	100													
r(C−C)	0.15	9	45	100												
r(C−H)	0.08	9	−4	9	100											
r(Ga−C)	0.06	55	−29	5	1	100										
∠Ga−N−C	31.4	−69	28	−10	−7	−34	100									
∠N−C−C	27.0	−10	−10	−26	−8	1	29	100								
∠N−Ga−C	45.4	−18	−7	1	1	−12	−19	−32	100							
∠Ga−C−H	34.6	28	−10	9	1	−6	−23	−59	37	100						
ϕ(Ga−N−C_6−C_8)	151.	−19	15	−4	−3	−9	56	19	−30	−1	100					
ϕ(C_3−Ga−N−H)	298.	7	−10	6	3	6	−15	−1	−7	−5	−22	100				
ϕ(Ga−N−C_7−C_9)	152.	17	−10	8	5	3	−47	−36	50	30	−61	18	100			
l(Ga−C)	0.08	25	−30	20	12	10	−24	−3	−4	10	−10	8	7	100		
l(Ga···$C_{6,7}$)	0.66	−21	13	−3	−4	−6	41	39	−81	−60	14	8	−44	−2	100	
l(C···C)	0.46	14	2	−1	1	5	7	15	5	−6	15	1	−9	7	−1	100

[a] σ_{LS} is the standard deviation from the final least squares refinement.

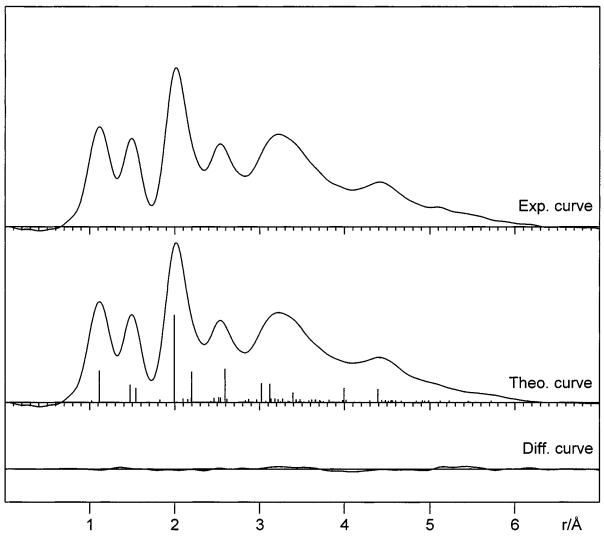

Figure 3. Radial distribution curves for $Me_3Ga{\cdot}NHEt_2$. The experimental curve is calculated from the average experimental intensity curve with theoretical data for $s \leq 1.75$ Å^{-1} and with convergence factor $B = 0.002$ Å^2. The vertical bars indicate the interatomic distances given in Tables 1 and 2; the lengths of the bars are proportional to the weights of the terms. The difference curve is experimental minus theoretical.

vibrational amplitudes. The correlation matrix for the refined parameters is given in Table 3. The final intensity and radial distribution curves are shown in Figures 2 and 3, respectively. Cartesian coordinates for the final model of $Me_3Ga{\cdot}NHEt_2$ are given in Table 3S in the Supporting Information.

Results and Discussion

The compound $Me_3Ga{\cdot}NHEt_2$ is readily prepared from the reaction of trimethylgallium and diethylamine as a colorless liquid with a vapor pressure of around 1 Torr under standard conditions. Samples of the adduct $Me_3Ga{\cdot}NHEt_2$ were characterized by ^{1}H NMR spectroscopy. The spectra obtained for the samples used in this study contained the expected four resonances. The resonances have been assigned by comparison with those of related compounds (Table 4) and with that of a sample reported previously.[8] From the integration ratios and the fact that only four resonances were observed, it was concluded that the desired adduct had been obtained in a pure form. The ^{1}H chemical shift for the methyl groups of trimethylgallium ($\delta = -0.20$) is upfield from TMS, indicating that a large shift in electron density from the nitrogen atom to the gallium atom occurs upon coordination. Schauer and Watkins found that ^{1}H and ^{13}C chemical shift values are displaced to lower fields with increasing steric bulk of the bound amine. The secondary amine $HNMe_2$ is the least sterically crowded of those studied and hence enjoys the largest upfield shift (^{1}H $\delta = -0.25$). This trend in downfield shift with increasing steric bulk was explained in terms of increasing p character of the M−C bond as the C−M−C bond angles decrease to accommodate the larger ligands.[8] Amines containing secondary carbons at the C(1) position cause a slightly smaller upfield shift of the methylgallium protons and ^{13}C atoms because of their greater bulk.

TABLE 4: ^{1}H NMR Data (ppm) for Me_3Ga Adducts[a]

compound	$\delta(-CH_3)$	$\delta(-CH_2)$	$\delta(-NH)$	$\delta(Me_3Ga)$
Me_3Ga				0.00s
$Me_3Ga.NMe_3$[38]	1.71s			−0.27
$Me_3Ga{\cdot}NMe_2H$[38]	1.61d		0.45s	−0.25
$Me_3Ga{\cdot}NEt_2H$[c]	0.54t	2.12dq	*b*	−0.20
$Me_3Ga.NEt_2H$[8]	0.57	2.13	0. 81	−0.18[d]
$[Me_2Ga{\cdot}NEt_2]_2$	0.66q	2.65q		−0.35

[a] s = singlet, d = doublet, t = triplet, dq = doublet of quartets. [b] No N−H resonance observed. [c] This work. [d] Relative to TMS.

The mass spectrum of $Me_3Ga{\cdot}NHEt_2$ contained no parent ion peak but showed peaks at 172 ($Me_2Ga{\cdot}NEt_2H^+$), 156 ($Me_2Ga{\cdot}NEtCH_2^+$ or $MeGa{\cdot}NEt_2H^+$), 141 ($Me_2Ga{\cdot}NEt^+$ or $Me_2Ga{\cdot}N(CH_2)_2^+$), 126 ($Me_2Ga{\cdot}NCH_2^+$ or $MeGa{\cdot}NEt^+$), 99 (Me_2Ga^+ or $MeGa{\cdot}NH^+$), 84 ($MeGa^+$), 68−73 (Ga^+ and NEt_2^+), and 57 ($NEtCH_2^+$). (For simplicity only peaks for ^{69}Ga are reported.) A mass spectral study of group 13 alkyls showed the Me_2M^+ ion to be the most abundant; thus the highest peak is assigned to $Me_2Ga{\cdot}NEt_2H^+$ rather than $Me_3Ga{\cdot}NHEtCH_2^+$.[32] The infrared spectra of $Me_3Ga{\cdot}NHEt_2$ obtained in the gas and solid phases (77 K) are given in Table 5, and assignments have been made on the basis of the comparison of the adduct spectrum with that of the free amine. Both the symmetric ν_s(Ga−C) and asymmetric ν_{as}(Ga−C) stretches were observed at wavenumbers close to those previously reported[8] and those reported for $Me_3Ga{\cdot}NHMe_2$.[25] The ν(Ga−N) vibration was observed as a weak band in the IR spectrum of the solid at 77 K at 429 cm^{-1} (cf. 433 cm^{-1} in $Me_3Ga{\cdot}NHMe_2$). The spectroscopic results indicate that $Me_3Ga{\cdot}NHEt_2$ can be transported in the vapor phase without decomposition, as can the methyl analogue, $Me_3Ga{\cdot}NHMe_2$.

Initial molecular orbital calculations indicated that the molecule could exist in a number of different conformations. However, calculations of vibrational frequencies ruled out the possibility of an AA or GG form and the most stable conformation for the molecule was found to be the AG form with torsion angles of +151° and −90 °. These were used as starting values in the least squares refinements. The more important values for

TABLE 5: Infrared Spectra of $Me_3Ga{\cdot}NHEt_2$ in the Gas and Solid Phases (77 K)

gas phase ν/cm^{-1}	77 K ν/cm^{-1}	approximate assignment
	3255 (m)	ν(N−H)
	3091	
2979 (s)	2981 (ms)	ν(C−H)
2968 (s)		ν(C−H)
2958 (s)		ν(C−H)
2948 (vs)	2938 (s)	ν(C−H)
2917 (ms)		ν(C−H)
2905 (ms)	2900 (m)	ν(C−H)
2896 (ms)		ν(C−H)
2876 (wm)		
1469 (wm)	1456 (m)	$\delta_{as}(CH_3)$ (N)
1391 (wm)	1390 (sh)	$\delta_s(CH_3)$
	1383 (m)	$\delta_s(CH_3)$
	1365 (w)	$\delta_s(CH_3)$
	1298 (w)	CH_2 wag
1247 (w)	1280 (w)	CH_2 twist
1202 (m)	1188 (ms)	$\delta_s(CH_3)$ (Ga), $\rho(CH_3)$ (N)
	1178 (m)	$\delta_s(CH_3)$ (Ga)
	1153 (w)	
1138 (wm)	1130 (m)	ν_{as}(C−N)
	1112 (wm)	$\rho(CH_3)$
	1087 (wm)	
	1070 (w)	
1054 (w)	1049 (wm)	ν(C−C)
	1031 (w)	
969 (m)	998 (m)	
908 (m)	910 (w)	ν_s(C−N)
842 (w)	846 (wm)	$\rho(CH_2)$
	813 (w)	$\rho(CH_2)$
	792 (m)	
759 (ms)	781 (sh)	
730 (sh)	729 (s)	$\rho(CH_3)$ (Ga)
	657 (m)	$\rho(CH_3)$ (Ga)
	566 (wm)	
550 (s)	544 (s)	ν_{as}(Ga−C)
514 (w)	513 (m)	ν_s(Ga−C)
	429 (w)	ν(Ga−N)

interatomic distances and angles are shown in Table 1 with a more extensive list of experimental values being contained in Table 2. Comparable distance and angle parameters from vapor-phase structural analyses on different gallium−nitrogen compounds are listed in Table 6. The Ga−N distance in $Me_3Ga{\cdot}NHEt_2$ (r_g = 2.204(12) Å) is the longest yet determined, which probably reflects the fact that this is the most sterically crowded gallium−nitrogen adduct yet investigated. Despite the length, and presumably weaker strength, of this Ga−N bond several gallium−nitrogen fragments were observed in the mass spectrum, indicating it is still a reasonably strong interaction. The Ga−C distance (r_g = 1.996(3) Å) is comparable with those found for $Me_3Ga{\cdot}NMe_3$ (r_a = 1.989(7) Å) and $Me_3Ga{\cdot}NHMe_2$ (r_g = 1.991(4) Å), but slightly longer than that in $Me_3Ga{\cdot}NH_3$ (r_g = 1.979(3) Å). Unsurprisingly, the Ga−C distance is markedly longer than that in the free Me_3Ga (r_g = 1.967(2) Å).[33] The N−C bonds in $Me_3Ga{\cdot}NHEt_2$ (r_g = 1.474(4) Å) and $Me_3Ga{\cdot}NHMe_2$ (r_g = 1.473(6) Å) are virtually identical in length and are also extended by the same amounts compared to values found in the free amines (1.464(1), 1.462(1) Å in $NHEt_2$;[34] 1.462(5) Å in $NHMe_2$[35]). It is noticeable that the ethyl group constrained in the gauche position ($C(7)H_2C(9)H_3$) attempts to relax steric crowding by increasing the Ga−N−C angle (115.5(9) Å) relative to that of the anti ethyl group (∠GaNC(6) = 109.6(9) Å). Significant differences were found between the three N−Ga−C(methyl) angles such that the Ga−C_3 fragment does not possess C_{3v} symmetry. The N−Ga−C(4) angle (102.8(3)°) is significantly larger than the other two equivalent angles. This could be a further consequence of the steric crowding imposed by the gauche ethyl group ($C(7)H_2C(9)H_3$). The C(4)···C(9) interaction (3.800(11) Å) is certainly shorter than the equivalent interaction with the anti ethyl group (C(5)···C(8) = 4.432(96) Å), and this steric effect is potentially responsible for the loss of symmetry of the $Ga(CH_3)_3$ group and the larger N−Ga−C(4) angle.

Thermolysis of $Me_3Ga{\cdot}NHEt_2$

It is well documented that amine adducts of group 13 methyl compounds undergo methane abstraction reactions, resulting in the formation of dimeric and sometimes trimeric species. The aim of this investigation was to determine if complete decomposition of the adduct would occur upon thermolysis, leaving gallium nitride, and thus to assess the potential of the compound as a single-source precursor to this material.

A sample of $Me_3Ga{\cdot}NHEt_2$ was heated to 180−200 °C under a pressure of nitrogen when dissociation commenced with evolution of a gaseous product. The gas was analyzed by IR and mass spectroscopy. Results from these analyses showed the gas to be methane. The residue was a colorless liquid, which was also investigated by mass spectroscopy and IR.

The highest peak observed in the mass spectrum of the residue was at m/e = 342 and showed a pattern indicative of the presence of two gallium atoms. This peak was assigned to the molecular ion, $[Me_2Ga{\cdot}NEt_2]_2^+$, suggesting that methane elimination had occurred with the formation of a dimeric product. A second, more intense peak, was observed at m/e = 327, which could be attributed to $[MeGa{\cdot}NEt_2][Me_2Ga{\cdot}NEt_2]^+$ or $[Me_2Ga{\cdot}NEtCH_2][Me_2Ga{\cdot}NEt_2]^+$. Evidence for the persistence of a four-membered Ga−N−Ga−N ring is obtained from the features observed in the mass spectrum in the m/e region 175−350. The spectrum of the residue in this region contains a number of features, all of which, we believe, are due to the presence of two gallium atoms. These features show the characteristic pattern, which arises from a dimeric gallium unit containing ^{71}Ga and ^{69}Ga isotopes in the approximate ratio 2:3.

The IR spectrum of the decomposition product at 77 K shows the main peaks of the methyl and ethyl groups and closely resembles that of the monomer in the region 1500−900 cm^{-1}. The main difference between the IR spectrum of the adduct and its decomposition product is the loss of the stretch assigned due to ν(N−H). The weak band assigned to ν(Ga−N), which occurs at 429 cm^{-1} in the spectrum of the monomer, is replaced by a stronger band at 459 cm^{-1} in the spectrum of the dimeric species. This stretch must now be due to a ring ν(Ga−N) mode.

TABLE 6: Bond Distances and Valence Angles in Some Ga−N Compounds[a,b]

	distance type	r(Ga−N)	r(Ga-X)	r(N−C)	∠N−Ga-X	∠X-Ga-X	∠Ga−N-X	ref
$Me_3Ga{\cdot}NH_3$	r_g	2.161(22)	1.979(3)		101.8(62)	115.9(42)	109.0[c]	20
$Me_3Ga{\cdot}NMe_3$	r_a	2.09(5)	1.989(7)	1.484(8)	99.3(2.2)	117.4	114.5(3.1)	36
$Me_3Ga{\cdot}NHMe_2$	r_g	2.170(13)	1.991(4)	1.473(6)	101.5(10)	116.4(7)	113.8(11)	25
$Me_3Ga{\cdot}NHEt_2$	r_g	2.204(12)	1.996(3)	1.474(4)	99.5(13)	117.3(8)	109.6(9)	*d*
$H_3Ga{\cdot}NMe_3$	r_a	2.139(4)	1.522(13)	1.479(3)	99.3(8)		115.5(9) 108.8(2)	37

[a] Distances (r_a or r_g) in Ångstroms, angles in degrees. [b] X = C or H. [c] Fixed. [d] This work.

In Table 4 are compared three resonances from the ^{1}H NMR spectra of $Me_3Ga{\cdot}NHEt_2$ and the decomposition product. The upfield shift of the methylgallium protons experienced in the ^{1}NMR spectrum of the decomposition product is to higher field ($\delta = -0.35$) than that of the monomeric 1:1 adduct ($\delta = -0.20$). This would be consistent with the formation of a dimeric compound in which the Ga−N bond may be shorter, as was found to be the case in $[Me_2Ga(\mu\text{-}NMe_2)]_2$ compared to $Me_3Ga{\cdot}NHMe_2$.

Taken together the spectral data are consistent with abstraction of methane from $Me_3Ga{\cdot}NHEt_2$ upon thermal decomposition and the formation of a dimeric $[Me_2Ga{\cdot}NEt_2]_2$ unit.

Thermal Decomposition of $[Me_2Ga{\cdot}NEt_2]_2$

Prolonged heating of $[Me_2Ga{\cdot}NEt_2]_2$ at 570−620 °C under an atmosphere of inert gas maintained at 200 °C resulted in evolution of methane and ethene, which were identified by gas-phase IR spectroscopy. Once the temperature reached 620 °C, the quantity of ethene produced increased and higher alkenes including but-1-ene were observed in the IR spectrum. Mass spectroscopic investigations carried out on the gaseous decomposition products supported the IR data and showed fragments that could be attributed to C_4H_8 and hexadienes ($m/e = 55, 78$). No volatile nitrogen-containing species were detected. The final involatile residue was a gray-green intractible solid and elemental analysis led to an empirical formula of $C_{3.3}H_{7.7}NGa_{1.6}$ showing that a large amount of organic material remains in the residue and that some undetected loss of nitrogen as volatile decomposition products had occurred.

The results suggest that the decomposition mechanism does not follow the path exhibited by $[Me_2Ga(\mu\text{-}NMe_2)]_2$, where both methane and dimethylamine were evolved. With $[Me_2Ga(\mu\text{-}NMe_2)]_2$ decomposition is thought to proceed via the initial breakage of a Ga−C bond followed by abstraction of a H atom to form methane. Eventual rupture of the Ga−N bond and the abstraction of a further hydrogen atom accounts for the formation of NMe_2H as a volatile product. With $[Me_2GaNEt_2]_2$ it is likely that decomposition proceeds via β-hydrogen elimination to produce ethene (i), followed by methane abstraction (ii).

$$[(CH_3)_2GaNEt_2]_2 \rightarrow [(CH_3)_2GaNEtH]_2 + 2C_2H_4 \quad \text{(i)}$$

$$[(CH_3)_2GaNEtH]_2 \rightarrow 2CH_4 + [CH_3GaNEt]_2 \quad \text{(ii)}$$

The decomposition is evidently not straightforward, as witnessed by the nonstoichiometric nature of the residue and the presence of higher alkenes among the volatile products.

Conclusion

The gas-phase structure of the adduct formed between trimethylgallium and diethylamine has been studied by electron diffraction and ab initio calculations. The thermal decomposition of the adduct has been investigated and was found to proceed initially by methane abstraction with the formation of a dimeric $[Me_2GaNEt_2]_2$ species. Both the gaseous and less volatile decomposition products were investigated by various spectroscopic techniques to confirm their nature. Further investigations involving thermolysis of $[Me_2GaNEt_2]_2$ were inconclusive, but results seemed to suggest that the decomposition mechanism at elevated temperatures involves a β-hydrogen elimination within the amine with release of ethene followed by loss of a further methyl group from the gallium as methane.

Acknowledgment. We thank the University of Reading for the Award of the Wilkie Calvert Research Studentship to C.E.B. We are grateful to Snefrid Gundersen and Hans Vidar Volden at the University of Oslo for help with collecting the electron diffraction data. This work has been supported by the Research Council of Norway (Program for Supercomputing) through a grant of computing time.

Supporting Information Available: Tables of total scattered intensities (Table 1S), background subtracted intensities (Table 2S), and Cartesian coordinates (Table 3S) from the final electron diffraction refinements for $Me_3Ga{\cdot}NHEt_2$. Supporting Information is available free of charge via the Internet at http://pubs.acs.org.

References and Notes

(1) Neumayer, D. A.; Ekerdt, J. D. *Chem. Mater*. **1996**, *8*, 9.
(2) For recent comprehensive reviews see: (a) Morkoc, H.; Mohammad, S. N. *Science* **1995**, *267*, 51. (b) Morkoc, H.; Strite, S.; Gao, G.; Lin, M. E.; Sverdlov, B.; Burns, M. *J. Appl. Phys*. **1994**, *76*, 1363. (c) Mohammad, S. N.; Salvador, A. A.; Morkoc, H. *Proc. IEEE* **1995**, *83*, 1306. (d) Matsuoka, T.; Ohki, T.; Ohno, T.; Kawaguchi, Y. *J. Cryst. Growth* **1994**, *138*, 727.
(3) Jones, A. C. *J. Cryst. Growth* **1993**, *129*, 728.
(4) Coward, K. M.; Jones, A. C.; Steiner, A.; Bickley, J. F.; Pemble, M. E.; Boag, N. M.; Rushworth, S. A.; Smith, L. M. *J. Mater. Chem*., **2000**, *10*, 1875.
(5) Lake, C. H.; Schauer, S. J.; Krannich, L. K.; Watkins, C. L. *Polyhedron* **1999**, *18*, 879.
(6) Sun, H. S.; Wang, X. M.; Sun, X. Z.; You, X. Z.; Wang, J. Z. *Acta Crystallogr., Sect. C* **1996**, *52*, 1184.
(7) Sun, H. S.; Wang, X. M.; You, X. Z.; Huang, X. Y. *Polyhedron* **1995**, *14*, 2159.
(8) Schrauer, S. J.; Watkins, C. L.; Krannich, L. K.; Gala, R. B.; Gundy, E. M.; Lagrone, C. B. *Polyhedron* **1995**, *14*, 3505.
(9) Hill, J. B.; Eng, S. J.; Pennington, W. T.; Robinson, G. H. *J. Organomet. Chem*. **1993**, *445*, 11.
(10) Byers, J. J.; Pennington, W. T.; Robinson, G. H. *Acta Crystallogr., Sect. C* **1992**, *48*, 2023.
(11) Bradley, D. C.; Dawes, H. M.; Hursthouse, M. B.; Smith, L. M.; Thorntonpett, M. *Polyhedron* **1990**, *9*, 343.
(12) Atwood, D. A.; Jones, R. A.; Cowley, A. H.; Atwood, J. L.; Bott, S. G. *J. Organomet. Chem*. **1990**, *394*, C6.
(13) Gerstner, F.; Hausen, H. D.; Weidlein, J. *J. Organomet. Chem*. **1980**, *197*, 135.
(14) Neumayer, D. A.; Cowley, A. H.; Decken, A.; Jones, R. A.; Lakhotia, V.; Ekerdt, J. G. *Inorg. Chem*. **1995**, *34*, 4698.
(15) Kouvetakis, J.; Beach, D. B. *Chem. Mater*. **1989**, *1*, 476.
(16) Neumayer, D. A.; Cowley, A. H.; Decken, A.; Jones, R. A.; Lakhotia, V.; Ekerdt, J. G. *J. Am. Chem. Soc*. **1995**, *117*, 5893.
(17) Hashimoto, M.; Amano, H.; Sawaki, N.; Akasaki, I. *J. Cryst. Growth* **1984**, *68*, 163.
(18) Coates, G. E. *J. Chem. Soc*. **1951**, 2003.
(19) Krauss, C. A.; Toonder, F. E. *Proc. Natl. Acad. Sci. U.S.A.* **1933**, *19*, 292.
(20) Almond, M. J.; Jenkins, C. E.; Rice, D. A.; Hagen, K. *J. Organomet. Chem*. **1992**, *439*, 251.
(21) Almond, M. J.; Drew, M. G. B.; Jenkins, C. E.; Rice, D. A. *J. Chem. Soc., Dalton Trans*. **1992**, 5.
(22) Interrante, L. V.; Sigel, G. A.; Garbauskas, M.; Hejna, C.; Slack, G. A. *Inorg. Chem*. **1989**, *28*, 252.
(23) Sauls, F. C.; Interrante, L. V.; Jiang, Z. *Inorg. Chem*. **1990**, *29*, 2989.
(24) Atwood, D. A.; Jones. R. A.; Cowley, A. H.; Bott, S. G.; Atwood, J. L. *Polyhedron* **1991**, *10*, 1897.
(25) Almond, M. J.; Beer, C. E.; Rice, D. A.; Hagen, K. *J. Mol. Struct*. **1995**, *346*, 86.
(26) Ziel, W.; Haase, J.; Wegmann, L. *Z. Instrumentenk* **1966**, *74*, 84.
(27) Hagen, K.; Hobson, R. J.; Holwill, C. J.; Rice, D. A. *Inorg. Chem*. **1986**, *25*, 3659.
(28) Ross, A. W.; Fink, M.; Hildebrandt, R. *International Tables of X-ray Crystallography*; Kluwer: Dordrecht, The Netherlands, 1992; Vol. 4.
(29) Frisch, M. J.; Trucks, G. W.; Schlegel, H. B.; Gill, P. M. W.; Johnson, B. G.; Robb, M. A.; Cheeseman, J. R.; Keith, T.; Petersson, G. A.; Montgomery, J. A.; Raghavachari, K.; Al-Laham, M. A.; Zakrzewski, V. G.; Ortiz, J. V.; Foresman, J. B.; Cioslowski, J.; Stefanov, B. B.; Nanayakkara, A.; Challacombe, M.; Peng, C. Y.; Ayala, P. Y.; Chen, W.; Wong, M. W.; Andres, J. L.; Replogle, E. S.; Gomperts, R.; Martin, R. L.;

Fox, D. J.; Binkley, J. S.; Defrees,; D. J. Baker, J.; Stewart, J. P.; Head-Gordon, M.; Gonzalez, C.; Pople, J. A. *Gaussian 94*, revision D.4*;* Gaussian, Inc.: Pittsburgh, PA, 1995.

(30) Hedberg, L.; Mills, I. M. *J. Mol. Spectrosc.* **2000**, *203*, 82.

(31) Hedberg, K.; Iwasaki, M. *Acta Crystallogr*. **1964**, *17*, 529.

(32) Glocking, F.; Strafford, R. G. *J. Chem. Soc. A* **1971**, 1761.

(33) Beagley, B.; Schmidling, D. G.; Steer, I. A. *J. Mol. Struct*. **1974**, *21*, 437.

(34) Takeuchi, H.; Kojima, T.; Egawa, T.; Konaka, S. *J. Phys. Chem*. **1992**, *96*, 4389.

(35) Wollrab, J. E.; Laurie, V. W. *J. Chem. Phys.* **1968**, *48*, 5058.

(36) Mastryukov, V. S. *Zh. Strukt. Khim*. **1987**, *28*, 143.

(37) Brain, P. T.; Brown, H. E.; Downs, A. J.; Greene, T. M.; Johnsen, E.; Parsons, S.; Rankin, D. W. H.; Smart, B. A.; Tang, C. Y. *J. Chem. Soc., Dalton Trans*. **1998**, 3685.

(38) Jenkins, C. E. Ph.D. Thesis, University of Reading, 1991.